

Absence of thermalization for systems with long-range interactions coupled to a thermal bathPierre de Buyl,¹ Giovanni De Ninno,^{2,3} Duccio Fanelli,^{4,5} Cesare Nardini,^{4,6} Aurelio Patelli,⁴ Francesco Piazza,⁷ and Yoshiyuki Y. Yamaguchi⁸¹*Center for Nonlinear Phenomena and Complex Systems, Université libre de Bruxelles, B-1050, Brussels*²*Laboratory of Quantum Optics, Nova Gorica University, Nova Gorica, Slovenia*³*Sincrotrone Trieste, Trieste, Italy*⁴*Dipartimento di Fisica e Astronomia, Università di Firenze and INFN, Via Sansone 1, IT-50019 Sesto Fiorentino, Italy*⁵*Dipartimento di Energetica "Sergio Stecco," Università di Firenze, via S. Marta 3, 50139 Firenze, Italy*⁶*Laboratoire de Physique, ENS Lyon, Université de Lyon, CNRS, 46 Allée d'Italie, FR-69364 Lyon cédex 07, France*⁷*Université d'Orléans and Centre de Biophysique Moléculaire (CBM), Rue Charles Sadron, 45071 Orléans, France*⁸*Department of Applied Mathematics and Physics, Graduate School of Informatics, Kyoto University, Kyoto 606-8501, Japan*

(Received 11 November 2012; published 15 April 2013)

We investigate the dynamics of a small long-range interacting system, in contact with a large long-range thermal bath. Our analysis reveals the existence of striking anomalies in the energy flux between the bath and the system. In particular, we find that the evolution of the system is not influenced by the kinetic temperature of the bath, as opposed to what happens for short-range collisional systems. As a consequence, the system may get hotter also when its initial temperature is larger than the bath temperature. This observation is explained quantitatively in the framework of the collisionless Vlasov description of toy models with long-range interactions and shown to be valid whenever the Vlasov picture applies, from cosmology to plasma physics.

DOI: [10.1103/PhysRevE.87.042110](https://doi.org/10.1103/PhysRevE.87.042110)

PACS number(s): 05.20.-y, 05.70.Ln, 52.65.Ff

I. INTRODUCTION

In the recent past, several theoretical and experimental studies have been devoted to exploring dynamical and thermodynamic properties of long-range interacting systems (LRISs) [1]. In such systems, energy is not additive. This fact, together with a possible break of ergodicity, is at the origin of a large gallery of peculiar thermodynamic behaviors: The specific heat of LRISs can be negative in the microcanonical ensemble [2], and temperature jumps may appear at microcanonical first-order phase transitions. These systems also display remarkable nonequilibrium dynamical features. For example, it is well known that under particular conditions isolated LRISs may get trapped in long-lasting quasistationary states (QSSs), whose lifetime diverges with system size [3,4]. Importantly, when performing the limit $N \rightarrow \infty$ (N being the number of particles), the system remains permanently confined in QSSs [5,6]. As a consequence, for large long-range interacting systems, QSSs are directly accessible through experiment [7–9].

Until today, the large majority of studies aimed at elucidating the fundamental properties of LRISs have been carried out on isolated systems, i.e., under the assumption that the system properties are not influenced by the external environment. However, recognizing whether a nonequilibrium QSS is stable to an external perturbation is of great importance [10], from both a theoretical and an experimental point of view. A related fundamental problem concerns the mechanism through which a LRIS exchanges energy with the surroundings. These questions epitomize the main motivation of the present work.

The nonequilibrium dynamical properties of the LRISs in contact with a thermal bath have been studied for the first time only recently [11–13]. As a possible realization of thermal bath, these authors considered a large Hamiltonian system with nearest-neighbor interactions, coupled to a fraction of the spins in the system. They concluded that the coupling with

the bath introduces a new time scale in the evolution of the system: the weaker the coupling strength, the longer the system remains trapped in a QSS before relaxing to equilibrium.

At variance with the above studies, we investigate here the dynamics of a LRIS in long-range contact with an additional large system trapped in a QSS. This interaction scheme can be regarded as a more clear-sighted realization of a *thermal bath* for a LRIS, opening the way to applications in diverse fields such as cosmology and plasma physics. For example, one may think of the collisionless mixing between plasmas, or the operation of magnetic fusion devices for energy production or the merging of globular clusters to a self-gravitating galaxy. Furthermore, it is also tempting to speculate that our simple scheme could be somehow relevant for the self-consistent interaction between dark (the bath) and baryonic (the system) matter in the universe (see, e.g., Ref. [14]).

II. THE LONG-RANGE THERMAL BATH AND THE CANONICAL QSS

As a reference case, we have selected the Hamiltonian mean field (HMF) model [15], widely regarded as a prototype LRI system. The HMF model describes the one-dimensional motion of N rotators coupled through a mean field cosine-like interaction,

$$H = \frac{1}{2} \sum_{j=1}^N p_j^2 + \frac{1}{2N} \sum_{i,j=1}^N [1 - \cos(\theta_j - \theta_i)], \quad (1)$$

where θ_j is the orientation of the j th rotator and p_j its conjugated momentum. To monitor the evolution of the system, it is customary to introduce the magnetization M , an order parameter defined as

$$M = \frac{\|\sum_i \mathbf{m}_i\|}{N}, \quad \text{where } \mathbf{m}_i = (\cos \theta_i, \sin \theta_i). \quad (2)$$

The infinite-range coupling between rotators is responsible for the emergence of rather intriguing behaviors, including the existence of QSSs. In a QSS the system displays non-Gaussian velocity distributions, and it takes values of M different than those predicted by equilibrium thermodynamics [4,5,16].

Rigorous mathematical results [17] indicate that in the limit $N \rightarrow \infty$ the discrete HMF dynamics reduces to the continuum Vlasov equation

$$\frac{\partial f}{\partial t} + p \frac{\partial f}{\partial \theta} - V'(\theta) \frac{\partial f}{\partial p} = 0, \quad (3)$$

where $f(\theta, p, t)$ is the microscopic one-particle distribution function, $V(\theta)[f] = -M_x[f] \cos(\theta) - M_y[f] \sin(\theta)$, $M_x[f] = \int_{-\pi}^{\pi} \int_{-\infty}^{\infty} f(\theta, p, t) \cos \theta d\theta dp$, and $M_y[f] = \int_{-\pi}^{\pi} \int_{-\infty}^{\infty} f(\theta, p, t) \sin \theta d\theta dp$. The specific energy $h[f] = \iint (p^2/2) f(\theta, p, t) d\theta dp - (M_x^2 + M_y^2 - 1)/2$ is a conserved quantity. The Vlasov equation defines the natural framework to address the puzzle of QSSs' emergence [3,5]. Specifically, QSSs are connected to the stable stationary solutions of the Vlasov equation. This observation suggests a statistical mechanics approach, inspired by the seminal work of Lynden-Bell [18], to characterize analytically the QSS properties. Lynden-Bell's approach is based on the definition of a locally-averaged ("coarse-grained") distribution, yielding an entropy functional defined from first-principle statistical-mechanics prescriptions. By constrained maximization of such an entropy, one obtains closed analytical expressions for the single-particle distribution in the QSS regime [5,6]. As a natural consequence, the QSSs can be equally interpreted as equilibrium configurations of the corresponding continuous description [19]. Hence, the QSS thermal bath that we consider here corresponds to a magnetized equilibrium solution of the underlying Vlasov equation (3).

Let $f_B(\theta, p)$ be the normalized single-particle distribution that characterizes the QSS bath. Such a function is obtained as the stationary solution of the Vlasov equation (3) corresponding to a water-bag initial distribution, $f_0(p, \theta) = 1/[4\Delta\theta_B \Delta p_B]$ for $\theta \in [-\Delta\theta_B, \Delta\theta_B]$, $p \in [-\Delta p_B, \Delta p_B]$ and zero elsewhere. Note that the initial magnetization of the bath $(M_0)_B$ and its energy density e_b can be expressed in terms of $\Delta\theta_B$ and Δp_B , as $(M_0)_B = \sin \Delta\theta_B / \Delta\theta_B$ and $e_b = \Delta p_B^2 / 6 + 1/2[1 - (M_0)_B^2]$. This in turn implies that the initial water-bag profile is uniquely determined by $(M_0)_B$ and e_b , in agreement with the Lynden-Bell theory.¹

At this point, $t = 0$ in our discussion, another HMF system with water-bag profile is injected and let to evolve consistently with the bath. This system, S in the following, is described in terms of its associated single-particle distribution $f_S(\theta, p)$. Clearly the bath should be significantly larger than the system to which it is coupled. This can be accomplished through the following normalization condition:

$$\int f_S(\theta, p, t) d\theta dp = 1 - \int f_B(\theta, p, t) d\theta dp = \epsilon, \quad (4)$$

¹The Lynden-Bell theory provides a quantitatively correct description of macroscopic observables, such as the average QSS magnetization. Alternative approaches accounting explicitly for nonergodicity yield more accurate predictions [16].

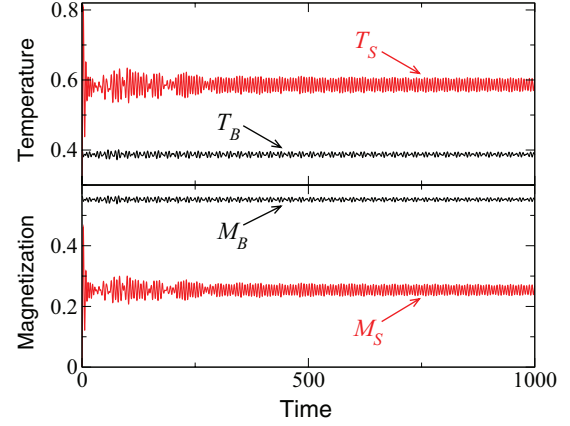


FIG. 1. (Color online) Time evolution of temperature and magnetization. The bath QSS originates from a water bag with energy 0.54 and initial magnetization 0.6. The system is initially homogeneous in space (i.e., zero magnetization), and its energy is set to 0.65. The coupling constant $\epsilon = 0.024$. All quantities are dimensionless.

where $\epsilon \ll 1$ sets the relative size of the two mutually interacting S and B HMF systems. We are interested in tracking the time evolution of the distribution $f(\theta, p, t) \equiv f_B(\theta, p, t) + f_S(\theta, p, t)$ under the constraint (4). From the physical point of view, we are reproducing the microcanonical dynamics of one isolated HMF system ($S + B$), composed of two subsystems supposed as distinguishable: The larger subsystem (the bath B) has already relaxed to its QSS equilibrium. The system S is initially confined in an out-of-equilibrium configuration of the water-bag type. To monitor the evolution of both subsystems, we follow the kinetic temperatures $T_\alpha(t) \equiv \Gamma_\alpha \int p^2 f_\alpha(p, \theta, t) d\theta dp$, with $\alpha = B, S$ and the corresponding magnetizations M_α . Here $\Gamma_S = 1/\epsilon$ and $\Gamma_B = 1/(1 - \epsilon)$. We emphasize that T_α are average kinetic energies per particle and not true thermodynamic temperatures. In fact, our results highlight the crucial fact that the appropriate definition of the true thermodynamic temperature associated with a QSS is not known.

A typical time evolution of these observables, obtained by numerical integration of the Vlasov equation (3), is illustrated in Fig. 1 [20]. Before *injecting* the system (i.e., at $t < 0$), the bath is first prepared in a water-bag initial condition and then allowed to evolve towards a QSS. After the bath has relaxed well into its QSS ($t = 0$), the interaction is switched on, meaning that a new HMF *combined system* is evolved, comprising bath and *system*. After a short transient, the system reaches a quasiequilibrium state where the mean value of the kinetic temperature is *different* from the temperature of the bath. In other words, the bath and the systems do not thermalize. Similarly, the two magnetizations converge to different values. Importantly, we note that the specific values of temperature and magnetization attained by the system spotlight a nontrivial interaction with the bath. T_S and M_S are indeed substantially different from the values that the system would reach when evolved microcanonically from the same initial condition. We obtain equivalent results upon simulating the discrete N -body dynamics (1). In this case, after a transient that gets progressively longer as the system size $N = N_S + N_B$ is increased, $\Delta T = T_B - T_S$ and $\Delta M = M_B - M_S$ tend to

zero. Thus, granularity causes thermalization, which is instead prevented in the continuum (Vlasov) limit. We term *canonical QSSs* the quasiequilibrium configurations that the system explores when in long-range contact with a QSS thermal bath in the zero energy-flux regime.

In the continuum limit, when the system is trapped in a canonical QSS, we find that the average energy flux between the bath and the system indeed vanishes, making the two subsystems by all means decoupled and thus preventing thermalization (see Appendix A for a more detailed analysis). It is remarkable that a zero-flux steady state is reached for $T_B \neq T_S$ in the noncollisional continuum limit, at variance with what is normally found in most collisional systems.

III. THE ENERGY FLUX BETWEEN THE SYSTEM AND THE BATH

Even more surprising is the behavior of the system during the “violent relaxation” stage towards the canonical QSS, which is characterized by a net energy flux from the (cold) bath to the (hot) system. To better illustrate this observation, we plot T_B and T_S versus time in Fig. 2. Note that T_S is larger than T_B at $t = 0$, the time of injection. As time progresses, the difference ΔT increases even further, resulting in an anomalous energy transfer from the bath to the system. In short, and counterintuitively, the *hot* system gets *hotter* when placed in contact with a large long-range QSS reservoir. This observation, although fighting intuition, does not violate any laws of physics, as the second law of thermodynamics is only expected to hold at thermal equilibrium.

Once the system has settled down in its canonical QSS at zero average energy flux, ΔT and ΔM are found to be different from zero. In order to pinpoint the relation between ΔT and ΔM , we performed a series of simulations for the same bath conditions as specified in the caption of Fig. 1, and varying the initial energy of the system S . Different energies lead to distinct canonical QSSs, as happens to isolated systems trapped in microcanonical QSSs. At first glance, it is tempting to speculate that canonical QSSs might originate from a net balance of two opposing thermodynamic forces, presumably related to ΔT and ΔM . However, we find that the dynamical

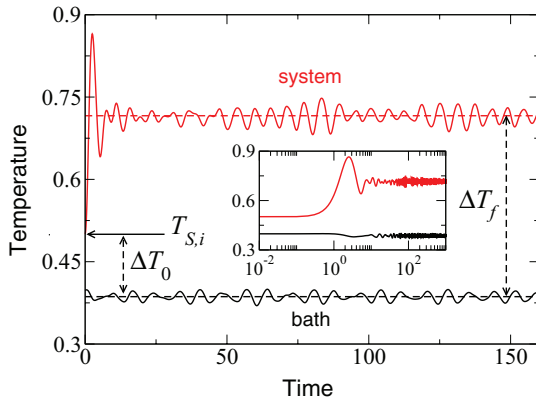


FIG. 2. (Color online) Bath and system temperatures versus time. The system is initially space homogeneous (zero magnetization) and has energy 0.75. Inset: Same plot with logarithmic time scale. Other parameters are as in Fig. 1. All quantities are dimensionless.

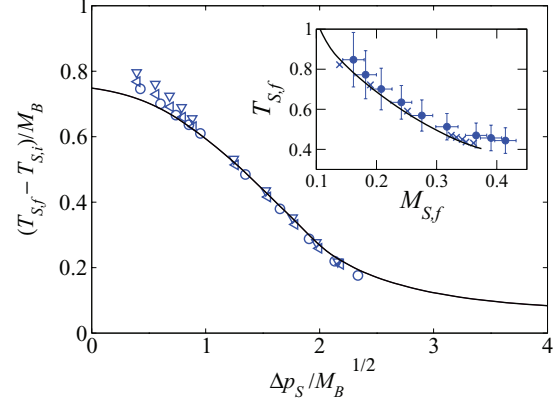


FIG. 3. (Color online) Difference between final and initial temperature of the system versus width of its initial water bag, in reduced units. Data refer to different choices of the bath parameters and to different initial energies of the (initially homogeneous) system. Symbols: Direct integration of Eqs. (5) for $M_B \in [0.1, 0.55]$, $T_B \in [0.3, 0.4]$. Solid line: Numerical solution of Eq. (8). Inset: $T_{S,f}$ vs $M_{S,f}$ for the same choice of parameters for the bath as in Fig. 1. Circles: N -body simulations (average over 100 independent realizations), $N_B = 4 \times 10^3$, $N_S = 10^2$. Crosses: Direct integration of the Vlasov equations. Solid line: Integration of Eq. (8). All quantities are dimensionless.

evolution of S is *not* influenced by the temperature of the bath T_B , at least for $\epsilon \ll 1$, but only responds to its magnetization M_B . Therefore, provided M_B is kept fixed, T_B can be set to an arbitrary value, without significantly altering the system dynamics. This is illustrated by the data collapse reported in Fig. 3.

IV. BEYOND THE HMF MODEL: A THEORETICAL INTERPRETATION BASED ON THE VLASOV EQUATION

This striking observation is unintuitive as compared to the case of short-range systems. Even more interestingly, it is by no means restricted to the HMF. In order to illustrate this fact, we note that in the Vlasov limit the distribution functions $f_\alpha(\theta, p, t)$ ($\alpha = B, S$) obey

$$\frac{\partial f_\alpha}{\partial t} + p \frac{\partial f_\alpha}{\partial \theta} - V'[f_B + f_S] \frac{\partial f_\alpha}{\partial p} = 0, \quad (5)$$

where $V(\theta)$ is a generic mean-field potential (the prime defining ordinary differentiation with respect to θ), defined as

$$V[f] = \int f(\theta', p', t) v(\theta - \theta') d\theta' dp', \quad (6)$$

$v(\theta - \theta')$ being the two-body potential. Since the system/bath relative size $\epsilon \ll 1$, we can treat it as a perturbative parameter, with $f_S \simeq O(\epsilon)$ and $f_B \simeq O(1)$. Expanding Eqs. (5) and keeping only terms that cause changes $\simeq O(\epsilon)$ in the physical observables, we are led to the two following coupled equations:

$$\frac{\partial f_\alpha}{\partial t} + p \frac{\partial f_\alpha}{\partial \theta} - V'[f_B] \frac{\partial f_\alpha}{\partial p} = 0, \quad \alpha = B, S. \quad (7)$$

The equation for the bath implies that this is frozen in its initial configuration, a stable equilibrium of the Vlasov equation,

$f_B(q, p, t) = f_B(q, p, t = 0)$ at all times.² The equation for f_S is the Liouville equation for a distribution of uncoupled particles moving in an external potential, f_B being constant. These conclusions are utterly general and should apply to any physical system whose density is governed by the Vlasov equation. For the HMF model, due to its rotational invariance, one has with no loss of generality

$$\frac{\partial f_S}{\partial t} + p \frac{\partial f_S}{\partial \theta} - M_B \sin \theta \frac{\partial f_S}{\partial p} = 0, \quad (8)$$

which is simply the Liouville equation for a set of uncoupled pendula. Hence, the leading-order evolution of f_S depends *only* on M_B and *not* on T_B . As is shown in Appendix B, M_B sets the width of the resonance of the pendulum along p , which scales as $\sqrt{M_B}$. This implies that the temperature should be proportional to M_B , as can be also appreciated by dividing Eq. (8) in the stationary state by $\sqrt{M_B}$.

Consistently with the above scaling arguments, we plot in Fig. 3 $(T_{S,f} - T_{S,i})/M_B$ as a function of the rescaled width of the initial water bag $\Delta p_S/\sqrt{M_B}$, for different values of the bath magnetization and temperature. The data refer to direct integration of the (constrained) Vlasov equations (5) and of Eqs. (8). In all cases, the data collapse nicely on a single master curve, which confirms the validity of our reasoning. An analytical calculation of $(T_{S,f} - T_{S,i})/M_B$ for $\Delta p_S = 0$ yields $(T_{S,f} - T_{S,i})/M_B \approx 0.751$, in excellent agreement with the result of direct integration of Eq. (8) (see Appendix B and Ref. [21]). The inset further shows that N -body simulations agree with all results obtained in the continuum limit.

V. CONCLUSIONS

Summarizing, we have proposed an implementation of long-range QSS bath. We showed that a small system in *true* long-range contact with a large, long-range reservoir reaches a zero-flux steady state, which we term *canonical* quasistationary state. These are stationary states of the system-bath coupled Vlasov equations, but quasistationary solutions of the associated N -body problem. Remarkably, in the explored range of parameters, we find that hotter-than-bath systems become hotter in canonical QSSs. In the context of the HMF model, based on simple scaling arguments, we have unveiled how the system anomalously increases its kinetic temperature as the fraction of its particles trapped in the resonance set by the bath magnetization gain energy. The kinetic energy gain is proportional to the value of M_B and independent of the bath temperature at the leading order in ϵ . We stress here, that this observation does not violate any fundamental laws of physics. Indeed, the average kinetic energy of the system does not coincide with its thermodynamic temperature. In this respect, our work raises the following central, yet unanswered, question: What is the correct thermodynamic measure of temperature for a system frozen in a QSS? Notice that in the present work, the energy of the thermal bath was chosen to lie in the part of the (microcanonical) phase diagram corresponding to a magnetized QSS. In regard to the system,

we considered initial energies leading to both magnetized and nonmagnetized (microcanonical) QSSs.

In conclusion, and based on the theoretical analysis that we have carried out, we argue that the results illustrated in this paper are general and extend beyond the HMF case study, whenever the collisionless Vlasov picture is a good description of the dynamics.

ACKNOWLEDGMENT

Discussions during the workshop ‘‘Equilibrium and out-of-equilibrium properties of systems with long-range interactions’’ held at the Centre Blaise Pascal, ENS-Lyon are acknowledged. F.P., D.F. and G.D.N. would like to thank D. Hane for insightful discussions.

APPENDIX A: THE ENERGY FLUX

The energy flux from the bath B to the system S is defined as $\Phi_{B \rightarrow S} = -dE_B/dt$, where E_B is the total energy of B . In order to derive an explicit expression for $\Phi_{B \rightarrow S}$, we start by calculating $\phi_j(t)$, the rate of energy loss of the j th particle. Denoting by h_j its energy, we have

$$\phi_j(t) \equiv -\frac{dh_j(t)}{dt} = -\frac{1}{2} p_j \mathbf{M} \cdot \mathbf{m}_j^\perp + \frac{1}{2} \frac{d\mathbf{M}}{dt} \cdot \mathbf{m}_j, \quad (A1)$$

where $\mathbf{m}_j \equiv (\cos \theta_j, \sin \theta_j)$ and $\mathbf{m}_j^\perp \equiv (-\sin \theta_j, \cos \theta_j)$, \mathbf{M} being the global magnetization

$$\mathbf{M} = (M_x, M_y) = \frac{1}{N} \sum_{j=1}^N \mathbf{m}_j. \quad (A2)$$

Here N is the total number of particles, i.e., the sum of those belonging to the bath, N_B , and those in the system, N_S . Summing over all particles belonging to the bath in Eq. (A1), one eventually obtains

$$\Phi_{B \rightarrow S} = \sum_{j \in B} \phi_j = -\frac{1}{2} \sum_{j \in B} p_j \mathbf{M} \cdot \mathbf{m}_j^\perp + \frac{N_B}{2} \frac{d\mathbf{M}}{dt} \cdot \mathbf{M}_B, \quad (A3)$$

where $\mathbf{M}_B = \sum_{j \in B} \mathbf{m}_j/N_B$ is the magnetization of the bath and the time derivative of \mathbf{M} reads

$$\frac{d\mathbf{M}}{dt} = \frac{1}{N} \sum_{j=1}^N p_j \mathbf{m}_j^\perp. \quad (A4)$$

In the continuum limit the sums are replaced by integrals

$$\Phi_{B \rightarrow S} = -\frac{1}{2} \int p \mathbf{M} \cdot \mathbf{m}^\perp(\theta) f_B(p, \theta) d\theta dp + \frac{1}{2} \frac{d\mathbf{M}}{dt} \cdot \mathbf{M}_B, \quad (A5)$$

where

$$\mathbf{M}_B = \int f_B \mathbf{m}(\theta) d\theta dp \quad \mathbf{M} = \int (f_B + f_S) \mathbf{m}(\theta) d\theta dp \quad (A6)$$

with $\mathbf{m}(\theta) = (\cos \theta, \sin \theta)$, $\mathbf{m}^\perp(\theta) = (-\sin \theta, \cos \theta)$.

According to the adopted sign convention, $\Phi_{B \rightarrow S}(t)$ is positive if the bath B cedes energy to the system. In Fig. 4 the instantaneous energy flux (upper panel) is plotted versus time

²A similar scenario is expected for baths at thermal equilibrium, which is also a stable state of the Vlasov equation.

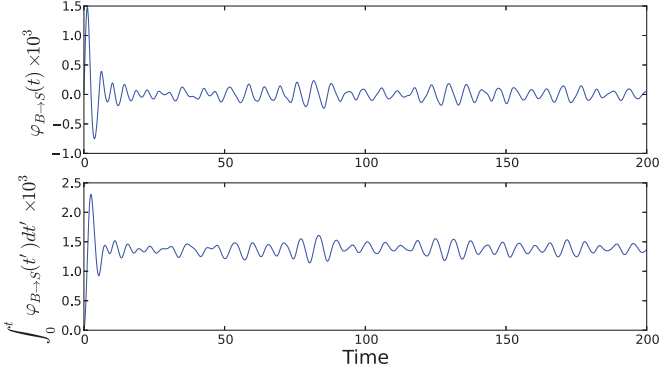


FIG. 4. (Color online) Time evolution of the instantaneous (top) and cumulated (bottom) bath-to-system energy flux. The system is initially space homogeneous and has energy 0.75. Other parameters are as in Fig. 1. All quantities are dimensionless.

for a typical realization of the Vlasov dynamics. After an initial transient, $\varphi_{B \to S}(t)$ oscillates around zero, implying that the bath B and the system S have established a zero-average-flux dynamical equilibrium. This condition corresponds to the emergence of the canonical QSS. Furthermore, the net energy flux is positive, a fact that can be appreciated by looking at the evolution of the cumulated flux (see lower panel of Fig. 4). This implies a net transfer of energy from the bath to the system.

We stress that the system gets hotter as its *total* energy increases after putting it in contact with the bath. The total energy of the system increases when it is put in contact with the bath, as is clearly proved by looking at the energy flux (the time derivative of the total energy) versus time in Fig. 4. The cumulated flux is positive, which, according to our conventions, attests to a flow of total energy from the bath to the system. In order to make this point even more clear, we show in Fig. 5 the total energy of the system versus time from the moment of the *injection*. The total energy of system and bath stays constant, while there is a clear flux of *total* energy

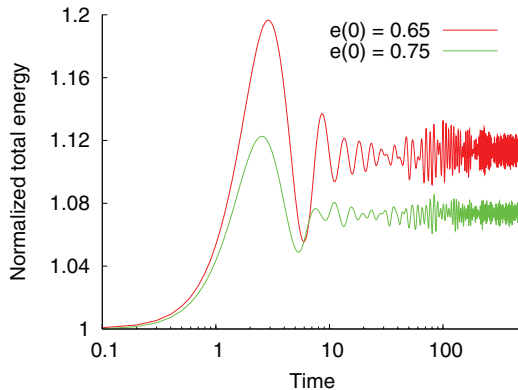


FIG. 5. (Color online) Total energy of the system in contact with a large reservoir in a QSS for two different initial energies, normalized by the $t = 0$ energy $e(0)$. The time $t = 0$ marks the moment where the system and the bath are put in contact. Following the injection, the combined (system + bath) ensemble is isolated, and hence its energy E_t stays constant. Other parameters are $M_0 = 0.6$ (initial magnetization of the bath), $E_t = 0.547$ [$e(0) = 0.65$], $E_t = 0.55$ [$e(0) = 0.75$]. All quantities are dimensionless.

from the bath to the tiny system, which is left permanently hotter as a result.

APPENDIX B: ON THE ANALYTIC ESTIMATE OF THE ASYMPTOTIC TEMPERATURE $T_{S,f}$

The phase space of the pendulum is foliated in trajectories with constant energy

$$e = \frac{p^2}{2} - M_B \cos \theta; \quad (\text{B1})$$

hence, $p(\theta) = \sqrt{2[e + M_B \cos \theta]}^{1/2}$. We want to discuss an analytic estimate of the quantity $(T_{S,f} - T_{S,i})/M_B$ for $\Delta p_S = 0$ and for an initial homogeneous system, $M_S(t = 0) = 0$. This calculation has the merit of enabling one to gain insight into the nature of the canonical QSS and further clarify the scaling adopted in Fig. 4. This analysis can be extended to cover the case $\Delta p_S \neq 0$, and also $M_S(t = 0) \neq 0$, a generalization to which we shall return in a separate contribution.

We note that $T_{S,i} = 0$ for $\Delta p_S = 0$. To evaluate $T_{S,f}$, we first consider the average kinetic temperature of the particles, which are assigned a given energy e . Here

$$\langle p^2 \rangle_e = \frac{1}{T(e)} \int_0^{T(e)} \dot{\theta}^2 dt, \quad (\text{B2})$$

where $\langle \cdot \rangle_e$ indicates a time average over one period,

$$T(e) = \frac{4}{\sqrt{M_B}} K \left(\frac{e + M_B}{2M_B} \right), \quad (\text{B3})$$

$K(\cdot)$ being the complete elliptic integral of the first kind. Expression (B2) takes the equivalent form

$$\langle p^2 \rangle_e = \frac{2}{T(e)} \int_{-\bar{\theta}(e)}^{\bar{\theta}(e)} p(\theta) d\theta, \quad (\text{B4})$$

where $\bar{\theta}(e) = \cos^{-1}(-e/M_B)$ is the angle of inversion of the selected (closed) trajectory. By performing the integral one eventually gets

$$\frac{\langle p^2 \rangle_e}{M_B} = \frac{2\sqrt{2(M_B + e)}}{\sqrt{M_B} K \left(\frac{e + M_B}{2M_B} \right)} E \left(\frac{\bar{\theta}(e)}{2}, \frac{2M_B}{e + M_B} \right), \quad (\text{B5})$$

where $E(\cdot, \cdot)$ is the incomplete elliptic integral of the second kind. The final temperature of the system can now be evaluated as

$$T_{S,f} \equiv \langle p^2 \rangle = \int_{-M_B}^{M_B} \langle p^2 \rangle_e \rho(e) de, \quad (\text{B6})$$

where $\rho(e)$ is the density of states of the system, which is univocally fixed by the initial condition. The integral in Eq. (B6) extends from $-M_B$ to M_B , i.e., the energies that identify the separatrix of the pendulum. In fact, the system is trapped inside the separatrix $|e| = M_B$, given the specific condition selected here ($\Delta p_S = 0$, hence no particle lies outside the resonance at $t = 0$). Recalling Eq. (B1), the distribution $\rho(e)$ can be calculated easily, as

$$\rho(e) = \frac{1}{\pi} \left| \frac{de}{d\theta} \right|^{-1} = \frac{1}{\pi} \frac{1}{\sqrt{M_B^2 - e^2}}. \quad (\text{B7})$$

Plugging Eq. (B7) into Eq. (B6) and recalling Eq. (B5), one eventually obtains

$$\frac{T_{S,f}}{M_B} = \sqrt{\pi} \int_{-1}^1 \frac{E(\cos^{-1}(-y)/2, \frac{2}{1+y})}{K(\frac{1+y}{2})} \frac{dy}{\sqrt{1-y^2}}. \quad (\text{B8})$$

Numerical integration gives $T_{S,f}/M_B \approx 0.751$, in excellent agreement with the data reported in Fig. 3. In the general case ($\Delta p_S \neq 0$), $e \propto \Delta p_S^2$. The scaling suggested by Eq. (B8) implies $\Delta p/\sqrt{M_B}$, which in turn explains the origin of the reduced variables used in Fig. 3.

-
- [1] A. Campa, T. Dauxois, and S. Ruffo, *Phys. Rep.* **480**, 57 (2009).
 [2] J. Barré, D. Mukamel, and S. Ruffo, *Phys. Rev. Lett.* **87**, 030601 (2001).
 [3] Y. Y. Yamaguchi *et al.*, *Physica (Amsterdam) A* **337**, 36 (2004).
 [4] A. Antoniazzi, D. Fanelli, J. Barre, P. H. Chavanis, T. Dauxois, and S. Ruffo, *Phys. Rev. E* **75**, 011112 (2007).
 [5] A. Antoniazzi, F. Califano, D. Fanelli, and S. Ruffo, *Phys. Rev. Lett.* **98**, 150602 (2007).
 [6] A. Antoniazzi, D. Fanelli, S. Ruffo, and Y. Y. Yamaguchi, *Phys. Rev. Lett.* **99**, 040601 (2007).
 [7] J. Barre, T. Dauxois, G. De Ninno, D. Fanelli, and S. Ruffo, *Phys. Rev. E* **69**, 045501(R) (2004).
 [8] R. Bonifacio and L. De Salvo, *Nucl. Instrum. Methods Phys. Res. A* **341**, 360 (1994).
 [9] R. Bachelard *et al.*, *J. Stat. Mech.* (2010) P06009.
 [10] C. Nardini *et al.*, *J. Stat. Mech.* (2012) L01002.
 [11] F. Baldovin and E. Orlandini, *Phys. Rev. Lett.* **96**, 240602 (2006).
 [12] F. Baldovin, P.-H. Chavanis, and E. Orlandini, *Phys. Rev. E* **79**, 011102 (2009).
 [13] P.-H. Chavanis, F. Baldovin, and E. Orlandini, *Phys. Rev. E* **83**, 040101 (2011).
 [14] V. Springel *et al.*, *Nature (London)* **435**, 629 (2005).
 [15] M. Antoni and S. Ruffo, *Phys. Rev. E* **52**, 2361 (1995).
 [16] Fernanda P. da C. Benetti, T. N. Teles, R. Pakter, and Y. Levin, *Phys. Rev. Lett* **108**, 140601 (2012).
 [17] W. Braun *et al.*, *Commun. Math. Phys.* **56**, 101 (1977).
 [18] D. Lynden-Bell, *Mon. Not. R. Astron. Soc.* **136**, 101 (1967).
 [19] F. Staniscia, A. Turchi, D. Fanelli, P. H. Chavanis, and G. De Ninno, *Phys. Rev. Lett.* **105**, 010601 (2010).
 [20] See Supplemental Material at <http://link.aps.org/supplemental/10.1103/PhysRevE.87.042110> for a movie depicting the time evolution of the bath and system phase portraits together with plots of the magnetization and the temperature.
 [21] P. de Buyl, D. Mukamel, and S. Ruffo, *Phys. Rev. E* **84**, 061151 (2011).